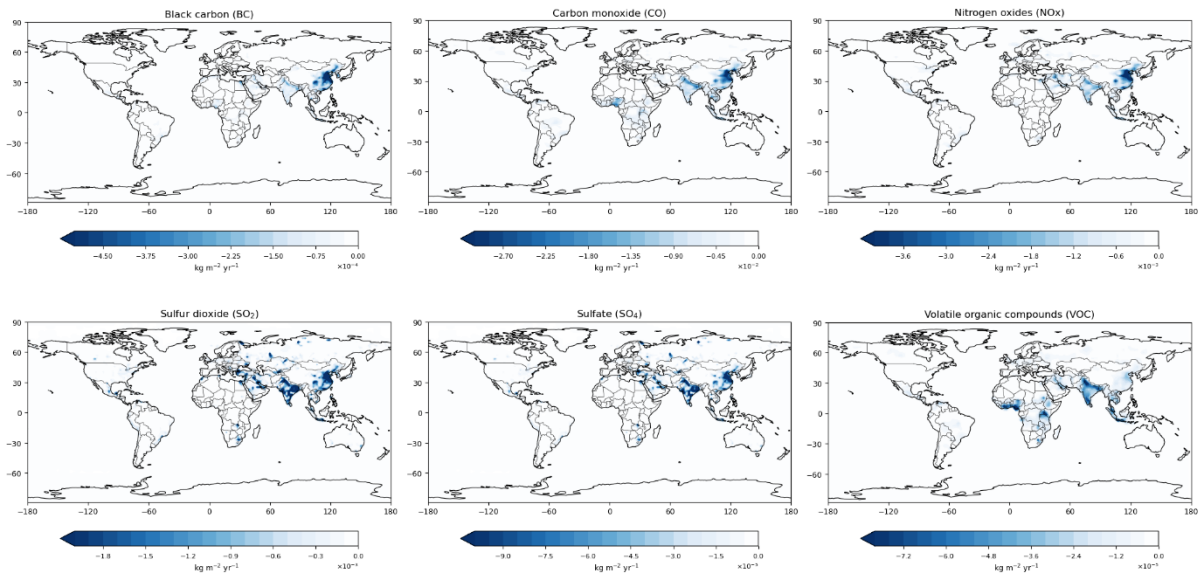
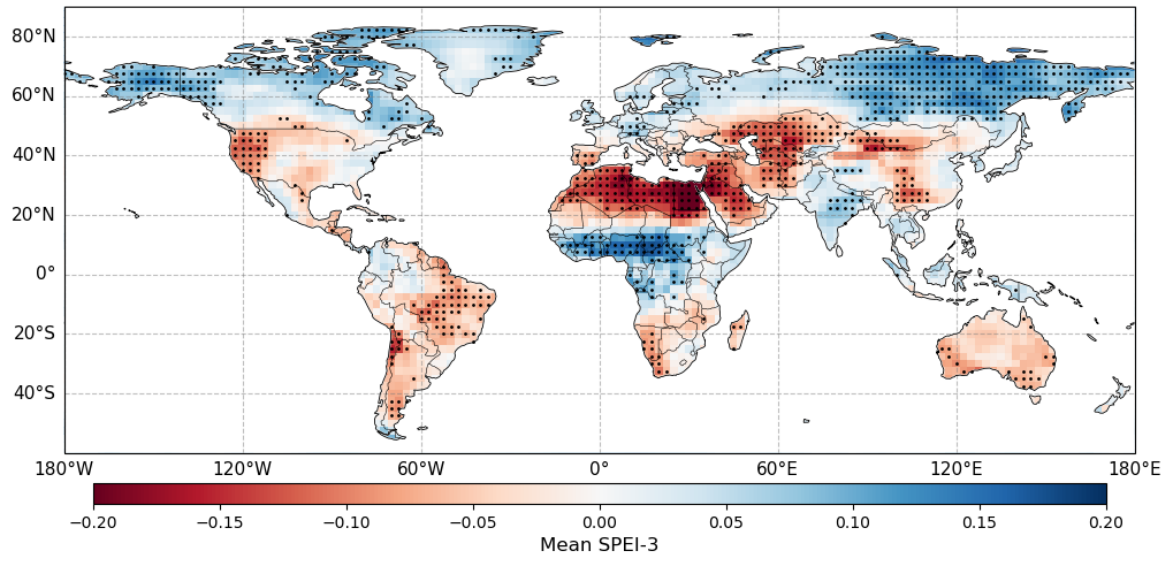


**Table S1. CMIP6 models analysed in this study.**

Name	Country	Resolution (latitude°×longitude°)	Realisations
BCC-ESM1	China	2.8×2.8	3
CNRM-ESM2-1	France	1.4×1.4	3
EC-Earth3-AerChem	Europe	0.7×0.7	3
MIROC6	Japan	1.4×1.4	3
MPI-ESM1-2-HAM	Germany	1.87×1.87	3
MRI-ESM2-0	Japan	1.1×1.1	3
UKESM1-0-LL	United Kingdom	1.3×1.9	3



**Figure S1: Spatial patterns of the differences in annual mean emission fluxes ( $\text{kg m}^{-2} \text{yr}^{-1}$ ) between SSP3-7.0-lowNTCF and SSP3-7.0 during 2036–2055 for BC, CO, NOx, SO<sub>2</sub>, SO<sub>4</sub>, and VOC.**



**Figure S2: Spatial pattern of annual mean MME SPEI-3 during the historical period (1995-2014). Black dots indicate grid cells where values are statistically significant from zero at the 95% level based on the Student's t-test.**

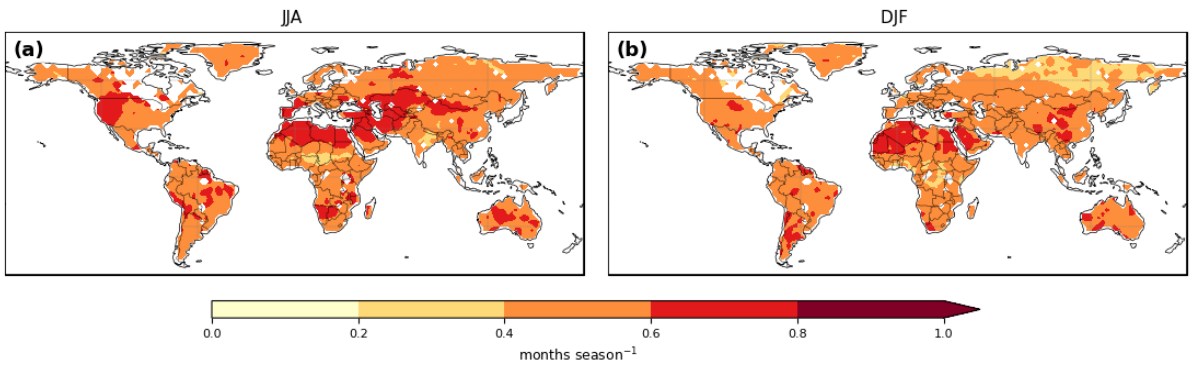


**Figure S3. Spatial patterns of MME drought occurrence (months season<sup>-1</sup>) during the historical period (1995-2014) for (a) JJA and (b) DJF**

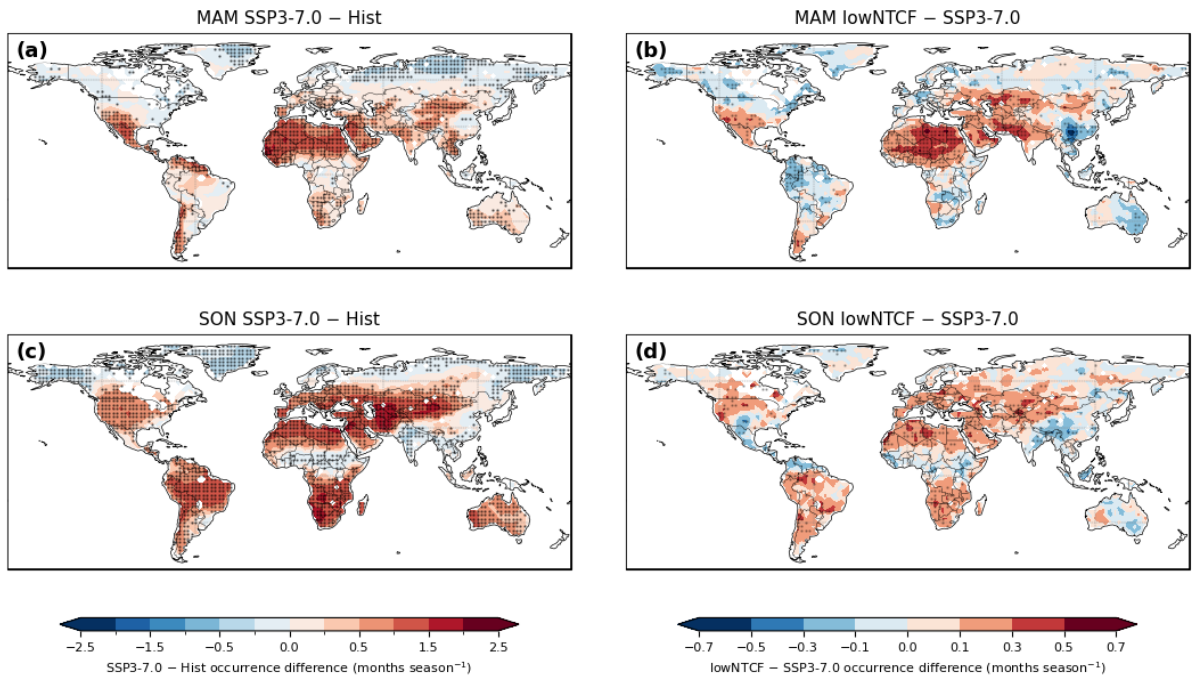


**Figure S4: (a) and (c): Spatial patterns of MME changes in drought occurrence (months season<sup>-1</sup>) under SSP3-7.0 during 2036-2055 relative to 1995-2014 for (a) MAM and (c) SON. (b) and (d): MME changes in future drought occurrence during 2036-2055 due to NTCF mitigation for (b) MAM and (d) SON. Stippling marks grid cells where the difference is statistically significant at the 90% level using a two-tailed Student's t-test.**

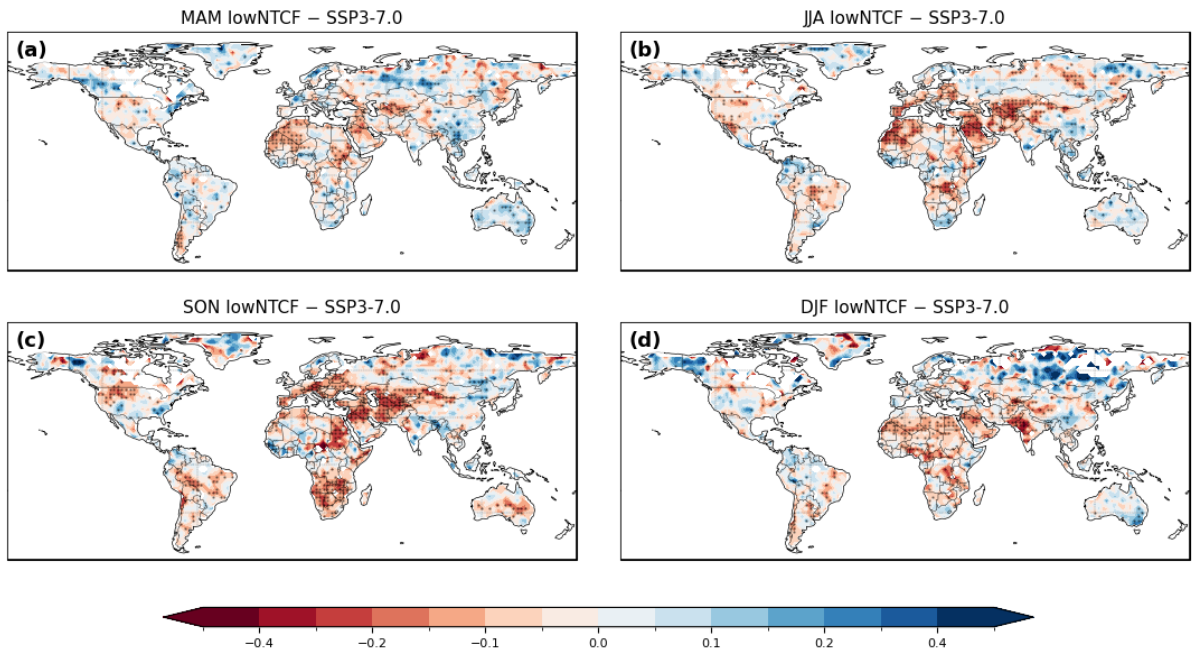


**Figure S5: Spatial patterns of MME changes in drought intensity (mean SPEI-3 per drought event) due to NTCF mitigation during 2036-2055 for (a) MAM, (b) JJA, (c) SON, and (d) DJF. Stippling marks grid cells where the difference is statistically significant at the 90% level using a two-tailed Student's t-test.**

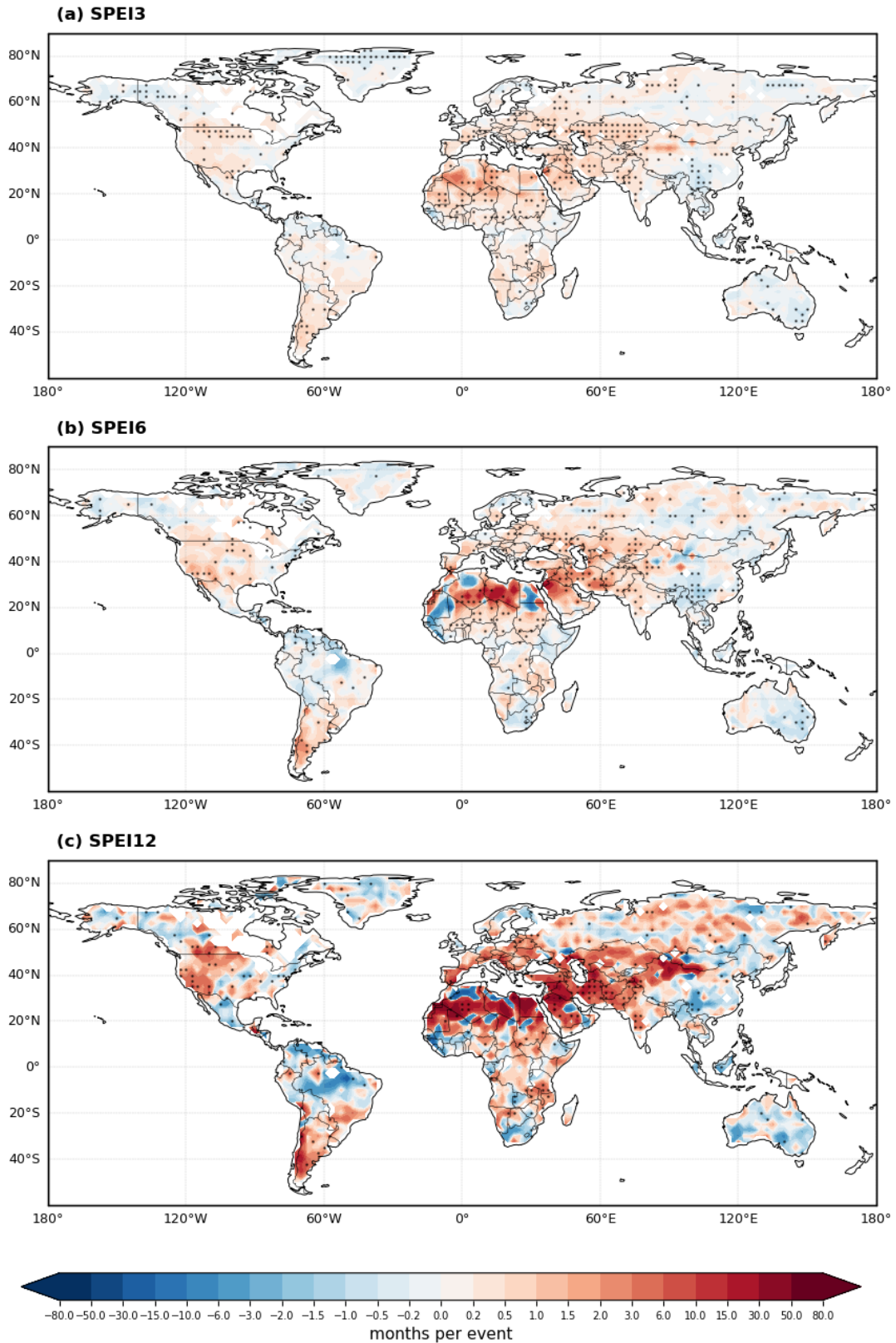


**Figure S6: Spatial patterns of MME changes in annual drought duration (months per event) due to NTCF mitigation during 2036-2055 for (a) SPEI-3, (b) SPEI-6, and (c) SPEI-12. Stippling marks grid cells where the difference is statistically significant at the 90% level using a two-tailed Student's t-test.**

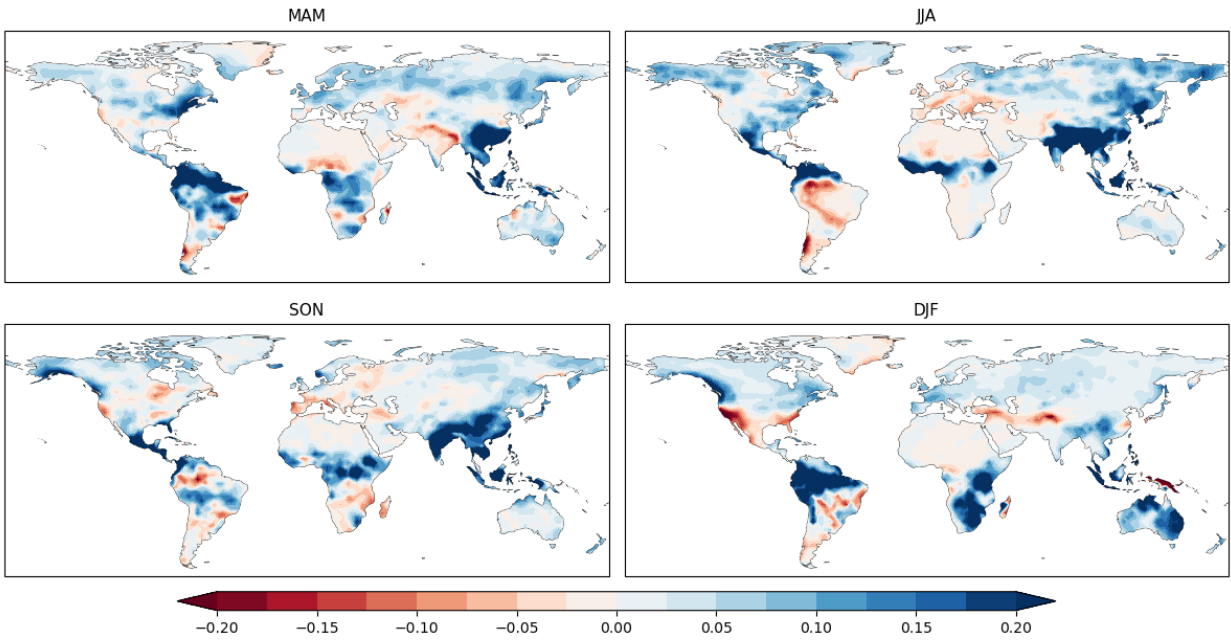


**Figure S7: Spatial patterns of seasonal MME changes in precipitation [mm day<sup>-1</sup>] during 2036-2055 due to NTCF mitigation.**

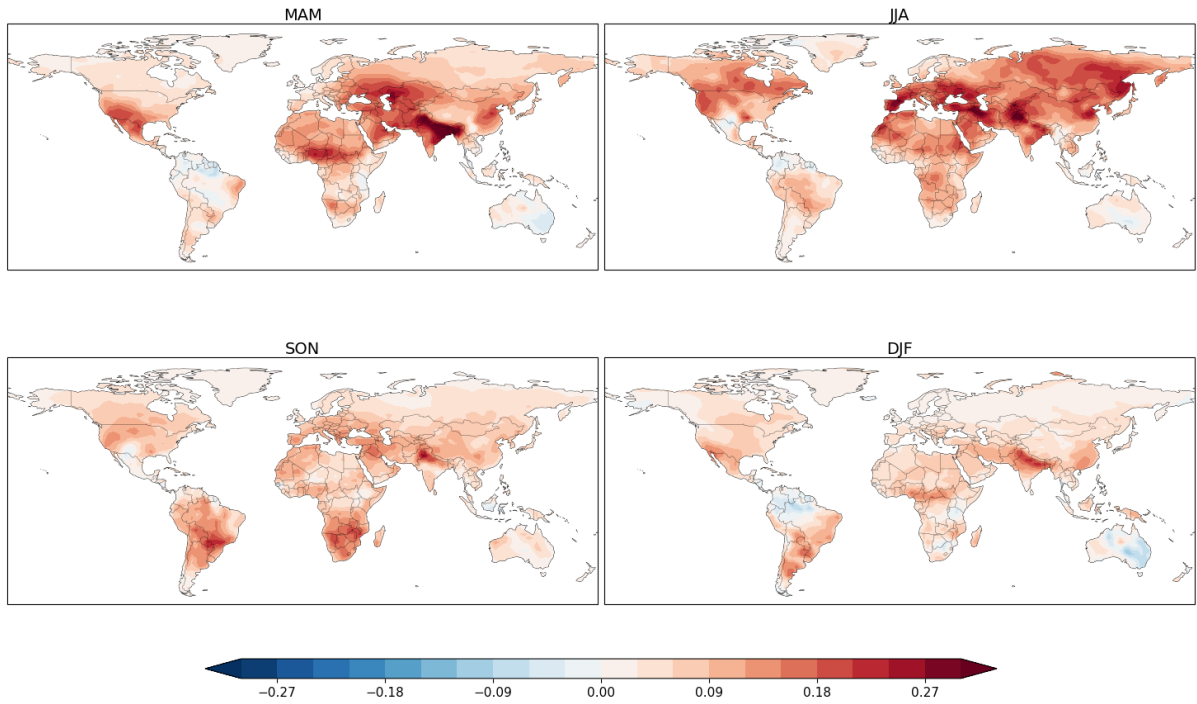


**Figure S8: Spatial patterns of seasonal MME changes in potential evapotranspiration [ $\text{mm day}^{-1}$ ] during 2036-2055 due to NTCF mitigation.**

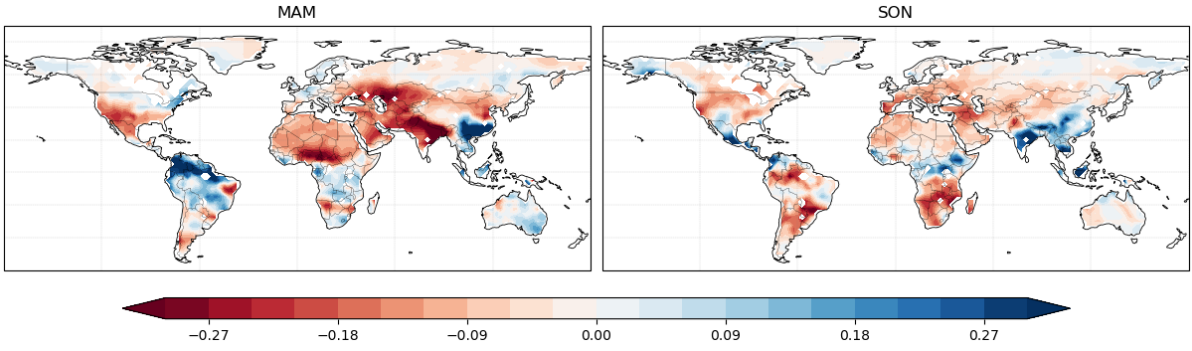


**Figure S9: Spatial patterns of MME changes in precipitation minus potential evapotranspiration ( $P - PET$ ) [ $\text{mm day}^{-1}$ ] for (left) MAM and (right) SON due to NTCF mitigation.**

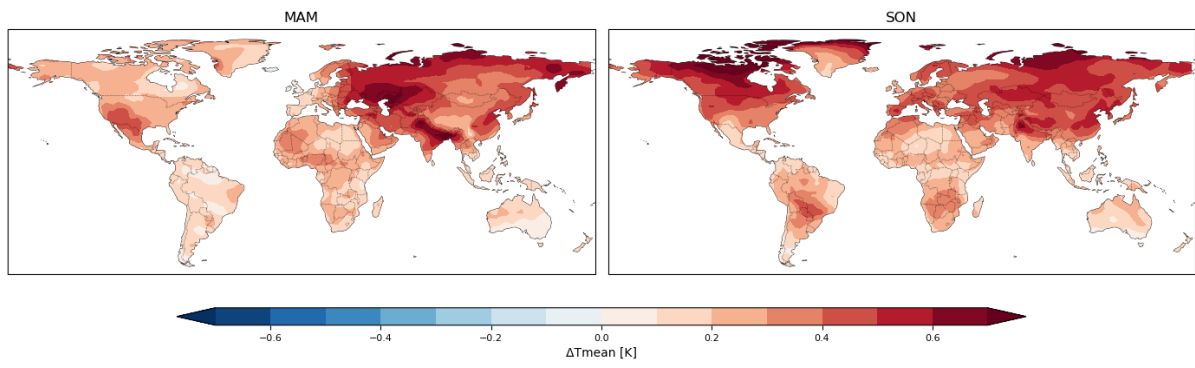


**Figure S10: Spatial patterns of MME changes in near-surface mean temperature ( $\Delta T_{\text{mean}} = (T_{\text{max}} + T_{\text{min}})/2$ ) [K] for (left) MAM and (right) SON due to NTCF mitigation.**

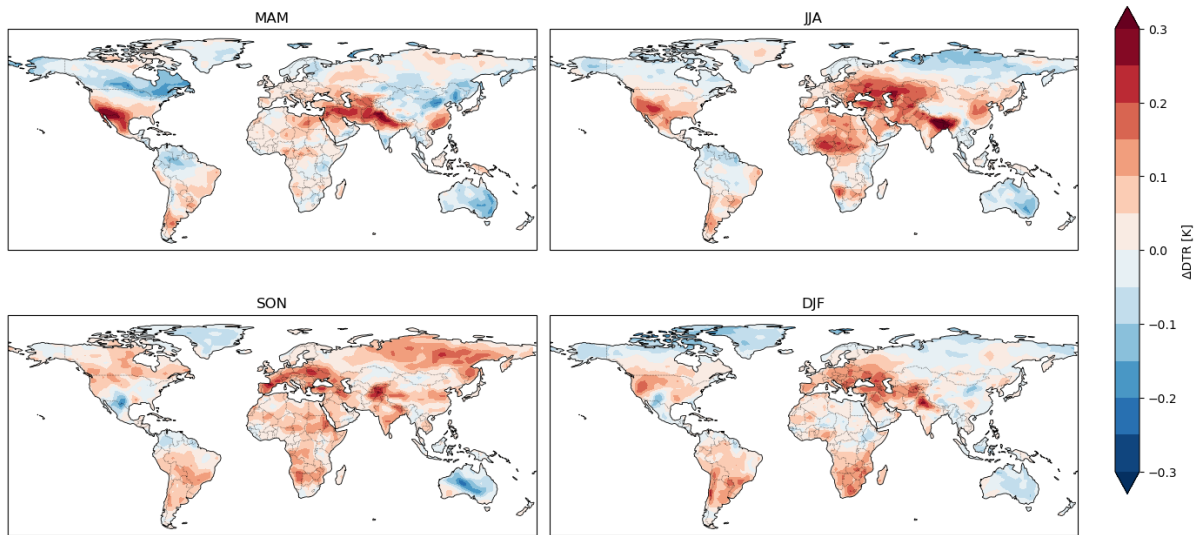


**Figure S11: Spatial patterns of seasonal MME changes in DTR ( $T_{max} - T_{min}$ ) [K] during 2036-2055 due to NTCF mitigation.**

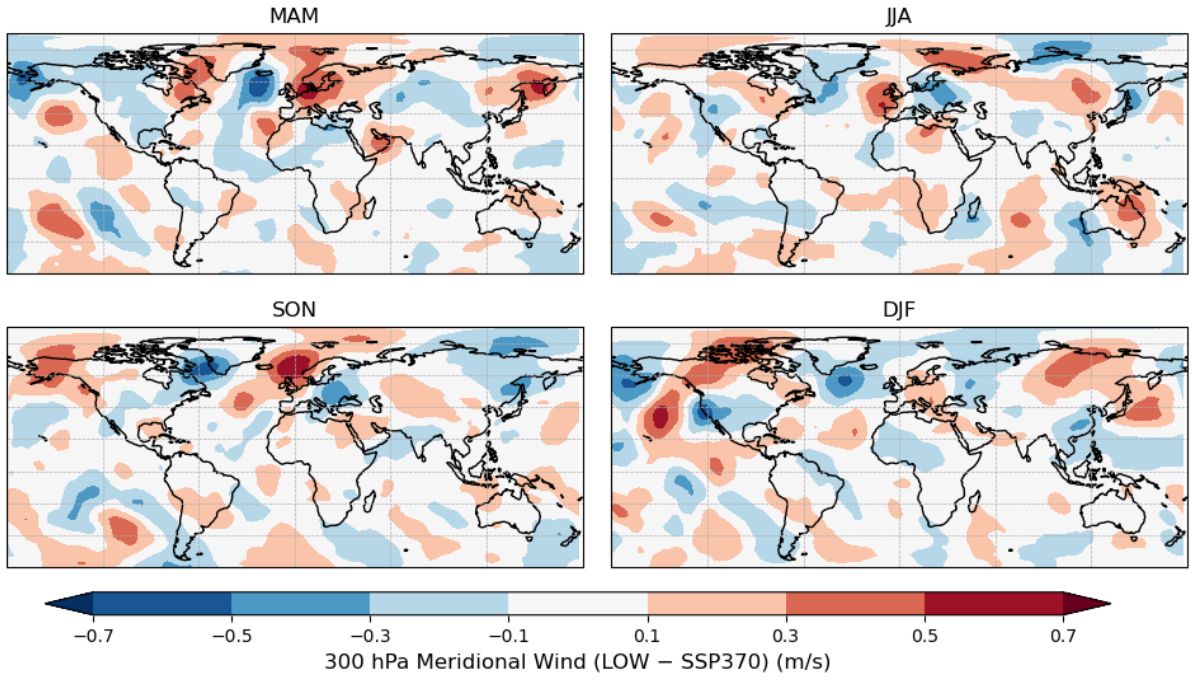


**Figure S12: Spatial patterns of seasonal MME changes in 300-hPa meridional wind [ $\text{m s}^{-1}$ ] during 2036-2055 due to NTCF mitigation.**

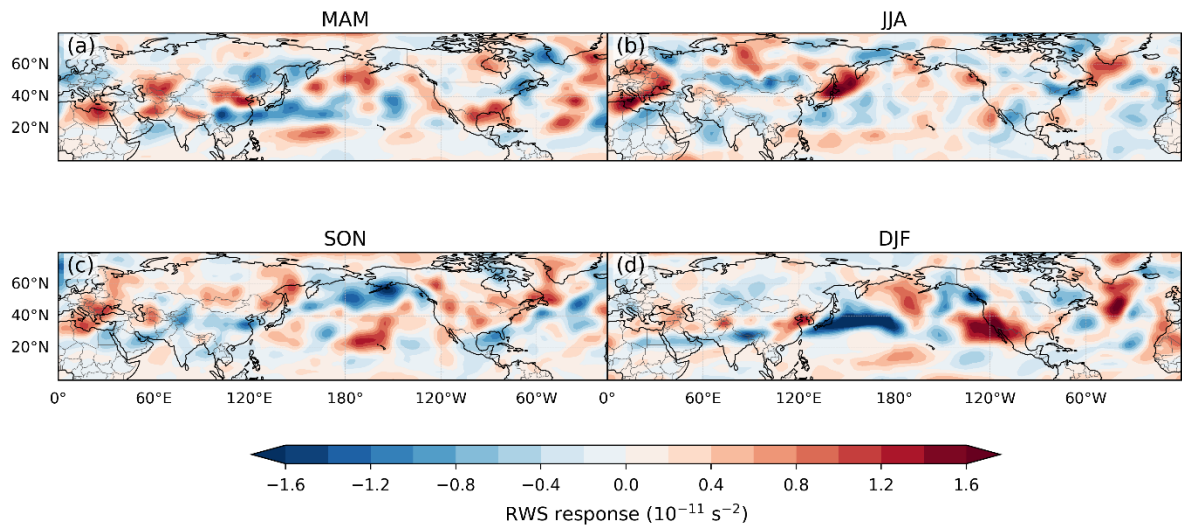


**Figure S13: Spatial patterns of seasonal MME changes in 200-hPa Rossby wave source [ $10^{-11} \text{ s}^{-2}$ ] during 2036-2055 due to NTCF mitigation.**

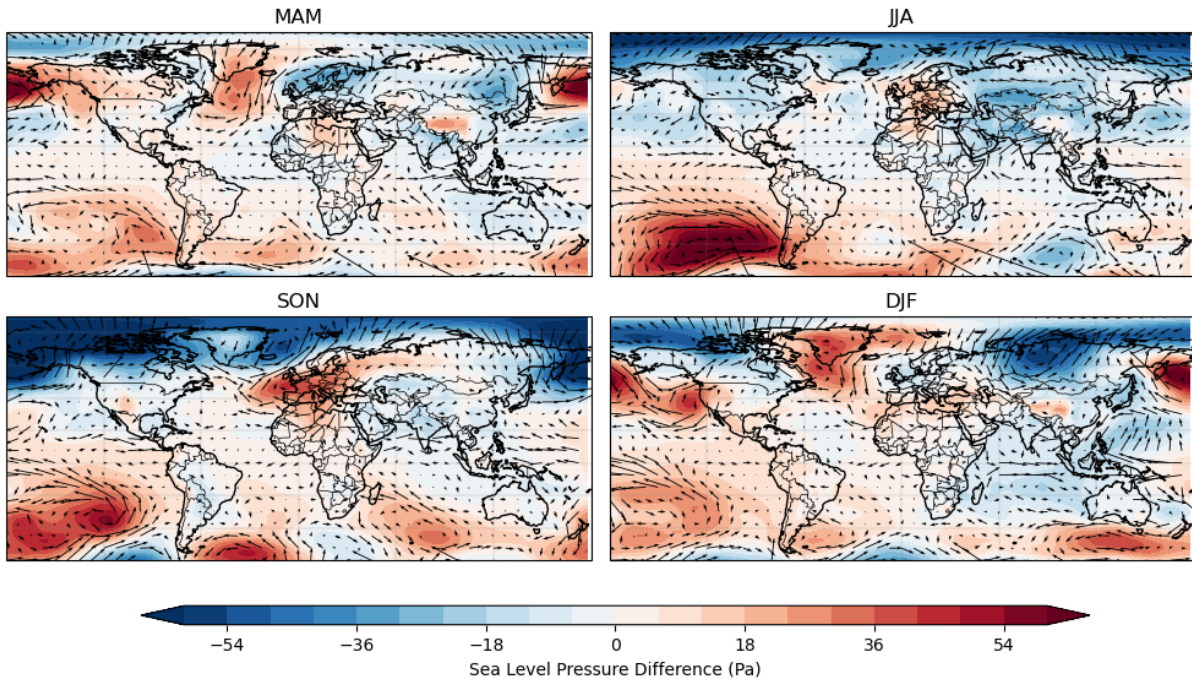


**Figure S14: Spatial patterns of seasonal MME changes in sea-level pressure [hPa] and 850-hPa winds [ $\text{m s}^{-1}$ ] during 2036-2055 due to NTCF mitigation.**

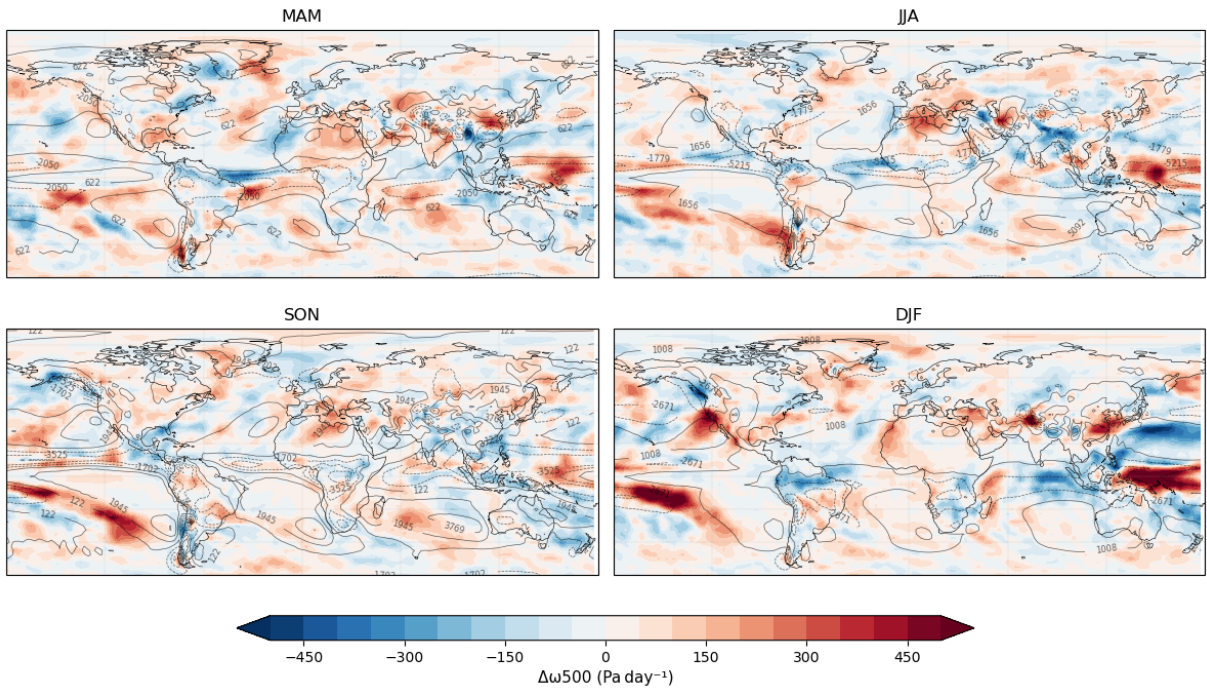


**Figure S15: Spatial patterns of seasonal MME changes in 500-hPa vertical velocity [Pa day<sup>-1</sup>] during 2036-2055 due to NTCF mitigation. Black contours represent the SSP3-7.0 climatological  $\omega_{500}$  values for reference.**

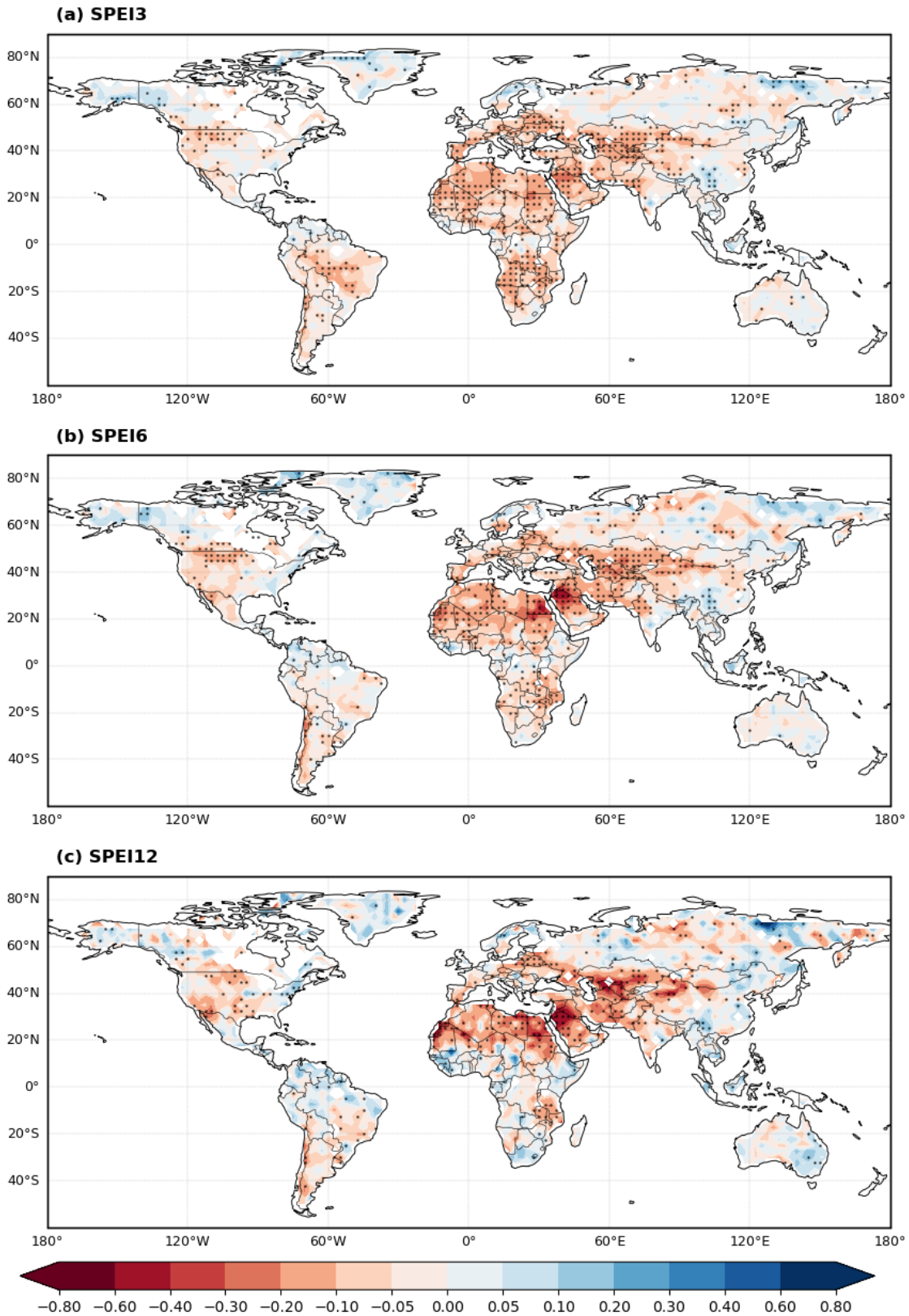


**Figure S16: Spatial patterns of MME changes in annual drought intensity due to NTCF mitigation during 2036-2055 for (a) SPEI-3, (b) SPEI-6, and (c) SPEI-12. Stippling marks grid cells where the difference is statistically significant at the 90% level using a two-tailed Student's t-test.**

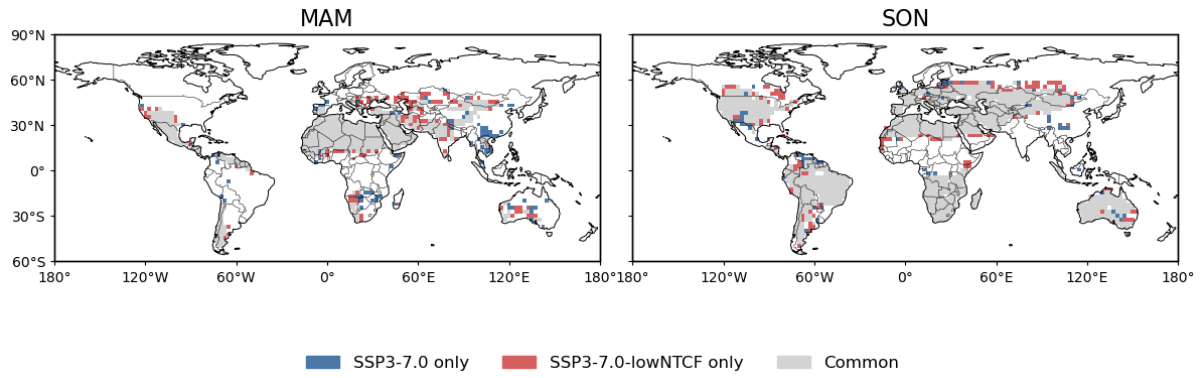


**Figure S17: MME changes in seasonal drought area during 2036–2055 for (left) MAM and (right) SON based on SPEI-3. A grid cell is defined as a drought area when at least two months within the season have  $\text{SPEI} \leq -1$  for at least five years during 2036–2055. Drought areas are shown only where at least five out of seven models agree on the sign. Blue indicates areas where drought occurs only under SSP3-7.0, red indicates areas where drought occurs only under SSP3-7.0-lowNTCF, and grey indicates areas common to both scenarios.**

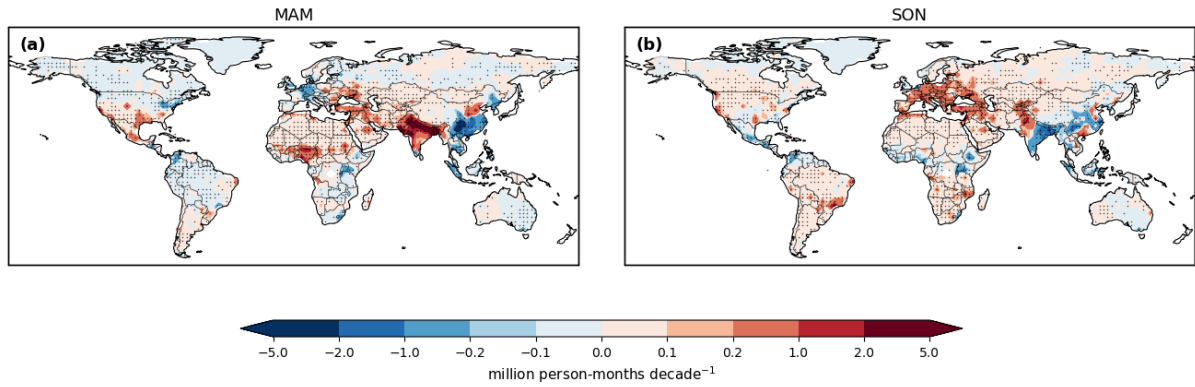


**Figure S18: Seasonal changes in gridded population exposure to drought under NTCF mitigation for (a) MAM and (b) SON during 2036–2055. Stippling indicates regions where at least 5 out of 7 models agree on the sign of the change. Values represent total population exposure within each  $2.5^\circ \times 2.5^\circ$  grid cell.**